International Journal of
Plasma Environmental Science and Technology

Regular Paper DOI: 10.34343/ijpest.2025.19.e01007

Particulate emission control for diesel engine by surface discharge electrostatic reactor

Kento Fukui[1], Kohei Kawakami[1], Apeksha Madhukar[2], Tomoyuki Kuroki[1], Haruhiko Yamasaki[1], Masaaki Okubo[1,*]

[1] Department of Mechanical Engineering, Osaka Metropolitan University, Japan
[2] School of Electrical Sciences, Indian Institute of Technology Goa, India

* Corresponding author: mokubo@omu.ac.jp (Masaaki Okubo)

Received: 25 December 2024
Revised: 20 February 2025
Accepted: 3 March 2025
Published online: 13 March 2025

Abstract

Diesel engines have better fuel economy and emit less CO_2 than gasoline engines. However, because their exhaust gas contains large amounts of nitrogen oxides (NO_x), particulate matter (PM), and hydrocarbons (HC), aftertreatment is necessary. We use a new plasma aftertreatment method to remove PM in the exhaust gas. Particle concentrations are measured before and after plasma treatment using a scanning mobility particle sizer (SMPS) and a laser particle counter (LPC). The engine load is set to 0%, 24%, 48%, and 72% using electric heaters. The exhaust gas is diluted with N_2+O_2 mixed gas (O_2 concentration 13%), and the mixed gas flow rate is adjusted to 5, 10, and 15 L min^{-1}. The input power of the reactor is adjusted to 100, 200, 300, and 400 W. PM removal performance is measured, and the removal efficiency is 83% or more under all conditions. At flow rates of 5 and 10 L min^{-1}, a removal efficiency of 95% or more is obtained. At a flow rate of 15 L min^{-1}, 48% load, and input power of 100W, a removal efficiency of 95% or more is obtained. At a flow rate of 15 L min^{-1}, the removal efficiency decreases under several conditions. Under these conditions, the residence time is short due to the high flow rate. It is also considered that sufficient removal is not achieved due to the large number of particles before treatment and the low discharge power. The increase in small particles reduces the removal efficiency in the small particle size range. Since previous studies have achieved high removal efficiencies of 67% NO_x and 76% HC using equipment and conditions similar to those of this device, we believe that this surface discharge electrostatic reactor can achieve highly efficient simultaneous removal of PM, NO_x, and HC.

Keywords: Diesel Engine, plasma, NO_x, PM, HC, simultaneous removal.

1. Introduction

Diesel engines have better fuel economy and lower CO_2 emissions than gasoline engines. However, diesel exhaust gas contains large amounts of NO_x, PM, and HC [1–6]. These substances are harmful to people's health and the environment. Therefore, when using diesel engines, it is important to perform aftertreatment. Currently, diesel particulate filters (DPFs), selective catalytic reduction (SCR), and HC/ NO_x trap catalysts are mainly used for aftertreatment. However, these methods have several disadvantages. DPFs have a large pressure loss and require regular regeneration to prevent clogging [7–17]. SCR requires regular catalyst replacement and a tank to store urea water [18]. HC/ NO_x trap catalysts cannot be used with heavy fuel oil [19]. In recent years, hybrid vehicles have become popular, and the use of electrical energy has been promoted in the automotive industry. The same is true for aftertreatment technology, and aftertreatment using plasma generated by electrical energy has attracted attention [20–36].

In this study, plasma is used to remove PM from diesel exhaust gas. PM is oxidized and removed using radicals generated by plasma. Previous research has shown that plasma exhaust gas treatment is effective not only for PM but also for NO_x and HC [37–39]. In other words, plasma aftertreatment technology is expected to be able to simultaneously remove NO_x, PM, and HC.

2. Experimental setup and methods

2.1 Experimental setup

Fig. 1 (a) shows a schematic diagram of a diesel engine exhaust gas treatment system using a plasma reactor. The exhaust gas from a diesel engine (YANMAR YDG250VS) collected from a sampling port passes through a drain pot. When the high-temperature exhaust gas passes through the drain pot, it is first cooled by the ice water surrounding the piping, and the water vapor in the exhaust gas is condensed into water. The water is stored in the drain pot, and the exhaust gas from which the water vapor has been removed flows out from the top of the drain pot. In this way, the water vapor in the exhaust gas is removed by passing through the drain pot, and the exhaust gas is cooled.

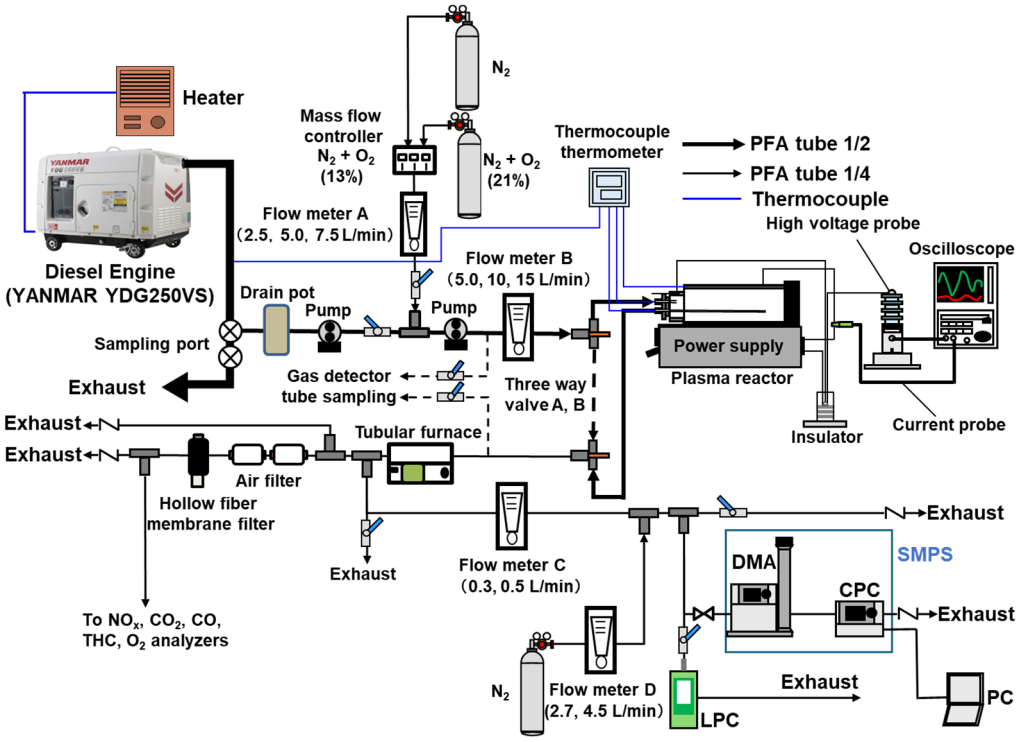

(a) Schematic of experimental setup.

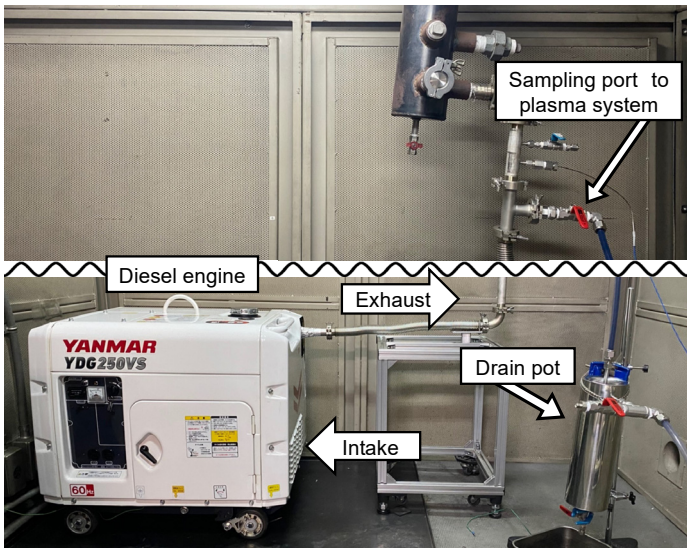

(b) Photograph of the diesel engine, exhaust piping, apparatus, and flow directions used in the experiment.

Fig. 1. Experimental setup for diesel exhaust treatment system using a surface discharge plasma reactor.

The engine load was set to 0%, 24%, 48%, and 72% for the experiments. Note that the gas temperatures before and after cooling, denoted as T_b and T_a, were as follows: T_b = 102 °C and T_a = 23°C at the engine load of 0%, T_b = 114 °C and T_a = 24 °C at the engine of 24%, T_b = 136 °C and T_a = 25 °C at the engine of 48%, and T_b = 149 °C and T_a = 25 °C at the engine of 72%. N_2 cylinder gas (secondary pressure fixed at 0.2 MPa) and synthetic air cylinder gas (N_2 = 79 %, O_2 = 21%, secondary pressure fixed at 0.2 MPa) are adjusted to an O_2 concentration of 13% using a mass flow controller (SFC280, Hitachi Metals, Ltd.). The flow rate of the dilution gas with an O_2 concentration of 13% is adjusted using flowmeter A (RK1710, KOFLOC Corp.; maximum flow rate = 5 NL min^{-1}) to dilute the exhaust gas by a factor of two (N: Standard state, 0 °C, 101.33 kPa). If the exhaust gas is not diluted, soot and moisture in the exhaust gas will adhere to the piping and trap PM. If PM is trapped, accurate experimental data cannot be obtained, or experiments cannot be performed, so dilution is performed. The dilution gas is N_2 + O_2 gas with an O_2 concentration of 13%, which is almost the same as the O_2 concentration of the exhaust gas and does not affect the reaction in the reactor. The mixed gas is transported by a pump (APN-110LVX1-2, Iwaki Co., Ltd.; maximum discharge pressure = 0.10 MPa) and adjusted to flow rates of 5, 10, and 15 L min^{-1} using flowmeter B (RK1710, KOFLOC Corp.; maximum flow rate = 20 L min^{-1}), and then fed into the plasma reactor for processing. Since O_3 is generated in the plasma reactor, the gas after the treatment contains O_3. Because O_3 may corrode or damage the measurement equipment, a tube furnace (KPO-14K, Isuzu Seisakusho Co., Ltd.) is installed immediately after the reactor, and pyrolysis is performed at a set temperature of 400 °C. Three-way valves A and B, shown in Fig. 1 (a), are installed to change the flow path so that exhaust gas would not flow into the reactor when the reactor is turned off, and moisture and particles would accumulate and adversely affect the measurement. After O_3 is decomposed, the gas is separated and flows into SMPS, LPC (HHCP3+, Beckman Coulter, Ltd.), and gas analyzers for NO_x (= NO + NO_2), NO, CO_2, CO, total hydrocarbon (THC), and O_2. Then, the flow rate is adjusted to 0.3 and 0.5 L min^{-1} using flowmeter C (RK1250, KOFLOC Corp.; maximum flow rate = 1 L min^{-1}), and sampling is performed. The sampled gas is diluted 10 times with N_2 (100%) cylinder gas (secondary pressure: 0.1 MPa) and measured by SMPS. The upper limit of particle number concentration in the measurement range of CPC is 2.5×10^5 cm^{-3}, so the gas is diluted with N_2 gas so as not to exceed this limit. A current probe (MODEL 2878, Pearson Electronics, Inc.; 10 A/V) and a high voltage probe 2000V/V (HV-P60, Iwatsu Electric Co., Ltd.; 2 kV/V) are also used. In addition, the exhaust gas temperature, the reactor wall temperature, the gas temperature before the reactor treatment, and the gas temperature after the reactor treatment are each measured using a temperature logger (SK-L400T, manufactured by Sato Keiryoki Seisakusho) connected to a K thermocouple sensor.

Fig. 1 (b) shows a photograph of the diesel engine, exhaust piping, apparatus, and flow directions used in this experiment. The diesel engine exhaust gas obtained from the sampling port has a high temperature and contains water vapor, which is removed and cooled by passing it through a drain pot.

2.2 Plasma treatment system

Fig. 2 (a) shows a schematic of the cylindrical surface discharge element and a cross-section of the inner wall of the element. The exhaust gas flows in through the sample inlet and flows out through the sample outlet after being treated with plasma. The equipment consists of a surface discharge tube utilizing the surface discharge induced plasma chemical process (SPCP discharge tube: OC-70/AC, Masuda Research Inc.) technology and a high-frequency and high-voltage power supply (HC Ⅱ-70/2, input: voltage = three-phases 200 Vac, power = 1.5 kVA (50/60 Hz), output: peak-to-peak voltage = 14 kV (no electrical load), input power = 70−860 W, frequency = 9.9 kHz, Masuda Research Inc.).

Fig. 2 (b) shows the front view of the surface discharge element and the high-frequency and high-voltage power supply. The element is a ceramic tube (outer diameter = 80 mm; length = 300 mm) with a discharge electrode on its surface of the ceramic tube and an induction electrode inside the ceramic. A surface discharge is extended along the inner walls of the discharge electrode and ceramic tube by applying a high frequency and voltage between the two electrodes. Thus, a surface discharge plasma is generated on the surface of the discharge electrode, thereby producing reactive free radicals (active oxygen (O) and nitrogen (N)) with strong oxidation properties. The PM, HC, and NO_x in the exhaust gas react with these active oxygen species for their removal. Air cooling of the heat-dissipating fins attached to the outer wall of the ceramic tube prevents overheating of the surface discharge elements.

Fig. 2 (c) shows the results when the power is turned off, whereas Fig. 2 (d) shows the results when the reactor input power is 400 W. These images show that the discharge is generated along the electrodes on the ceramic surface.

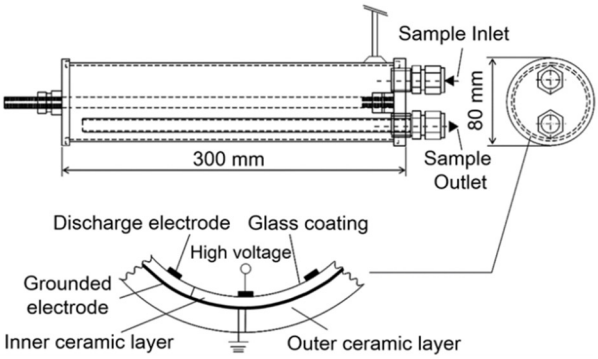

(a) Surface discharge element and cross-section of the inner wall of the element.

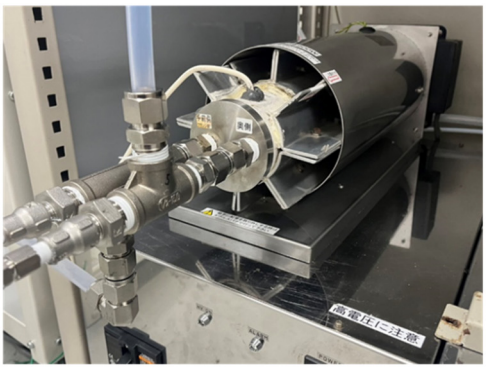

(b) Front view of the surface discharge element and the high-frequency and high-voltage power supply.

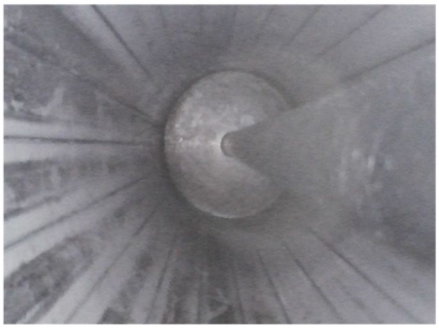

(c) Photograph inside the surface discharge plasma reactor when the power is turned off.

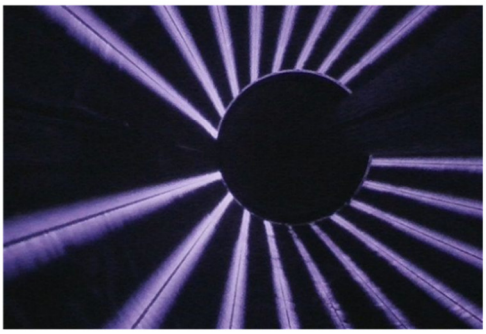

(d) Photograph inside the surface discharge.

Fig. 2. Surface discharge plasma reactor.

2.3 Experimental condition and measurement procedure

In the plasma reactor shown in Fig. 2, the input power to the reactor is set to 0, 100, 200, 300, and 400 W, and the particle removal efficiency and discharge power of the reactor are measured. It takes 10 minutes for the power to stabilize. First, check the flow rate and dilution. The engine load is 0%, 24%, 48%, and 72%, the flow rate is 5, 10, and 15 L min^{-1}, and the dilution ratio is two times. Wait for 10 minutes with the reactor OFF. For the first 5 minutes, the mixed gas does not pass through the reactor, and for the remaining 5 minutes, the flow rate is changed by the three-way valves A and B to pass the mixed gas through the reactor. The particle number is measured with the SMPS and LPC to obtain the particle number before treatment. Then, the reactor is turned on, and the power is left to stabilize for 10 minutes with the reactor on. Then, the particle number is measured with the SMPS and LPC to obtain the particle number before treatment. The discharge power is also measured using an oscilloscope. After the measurement is completed, the flow path is changed using three-way valves A and B so that the mixed gas does not pass through the reactor. Then, the power to the reactor is turned off. This operation is repeated three times, and this is considered as one measurement condition.

3. Results and discussion

3.1 Particle concentration

Fig. 3 shows the particle number concentration distribution of PM by size before and after treatment at different flow rates and engine loads. Fig. 3 (a) shows the results at a flow rate of 5 L min^{-1} and 0% load, Fig. 3 (b) shows the results at a flow rate of 5 L min^{-1} and 48% load, Fig. 3(c) shows the results at a flow rate of 10 L

min^{-1} and 0% load, Fig. 3(d) shows the results at a flow rate of 10 L min^{-1} and 48% load, Fig. 3 (e) shows the results at a flow rate of 15 L min^{-1} and 0% load, and Fig. 3 (f) shows the results at a flow rate of 15 L min^{-1} and 48% load. The horizontal axis shows particle size (mobility diameter) (nm), and the vertical axis shows particle number concentration (dN/dlog D_p (cm^{-3})). Q is the gas flow rate after plasma treatment, Q_A is the sampling flow rate from the engine, Q_C is the gas flow rate during particle measurement, and Q_D is the dilution gas flow rate.

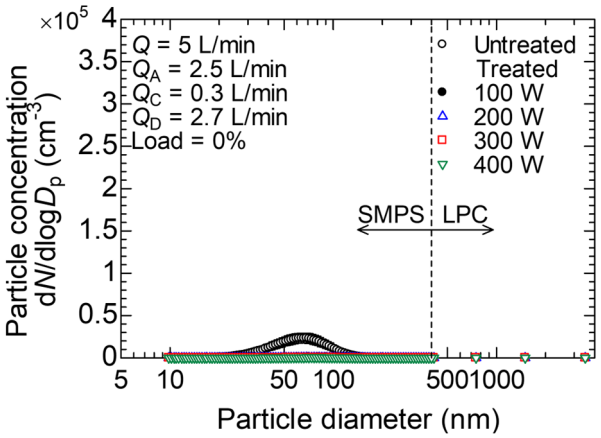

(a) flow rate Q of 5 L/min, engine loads of 0 %.

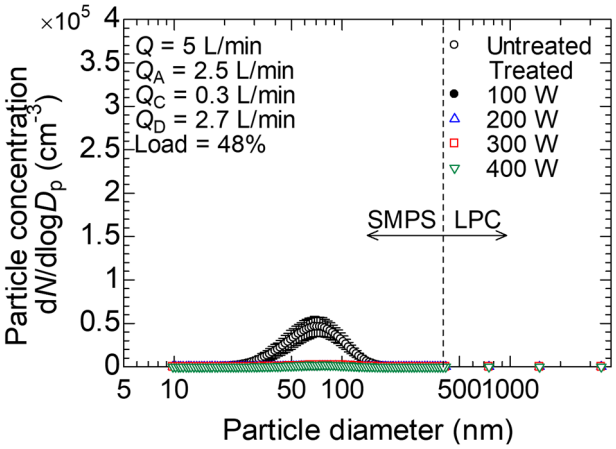

(b) flow rate Q of 5 L/min, engine loads of 48 %.

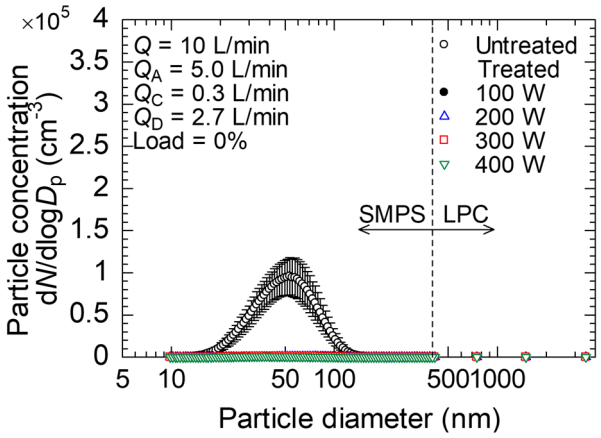

(c) flow rate Q of 10 L min^{-1}, engine loads of 0 %.

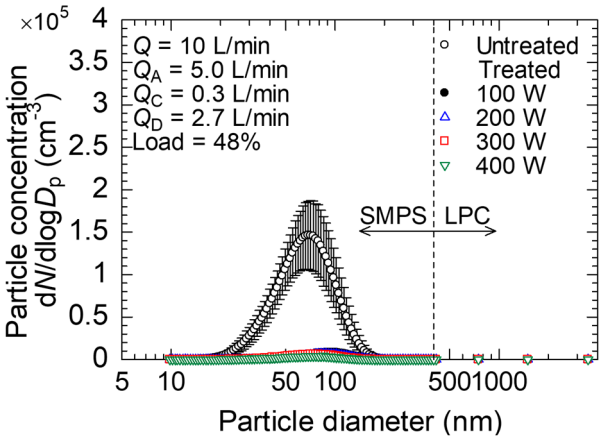

(d) flow rate Q of 10 L min^{-1}, engine loads of 48 %.

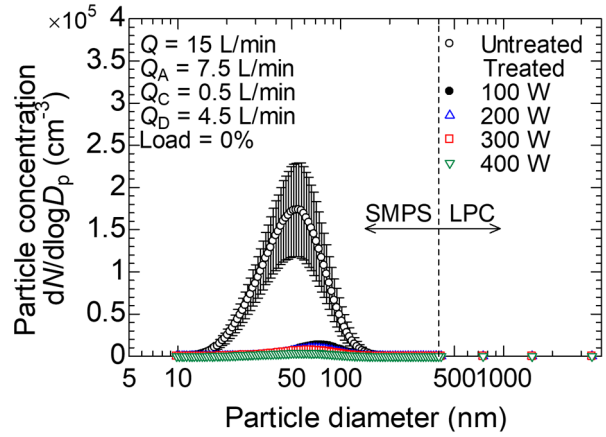

(e) flow rate Q of 15 L min^{-1}, engine loads of 0 %.

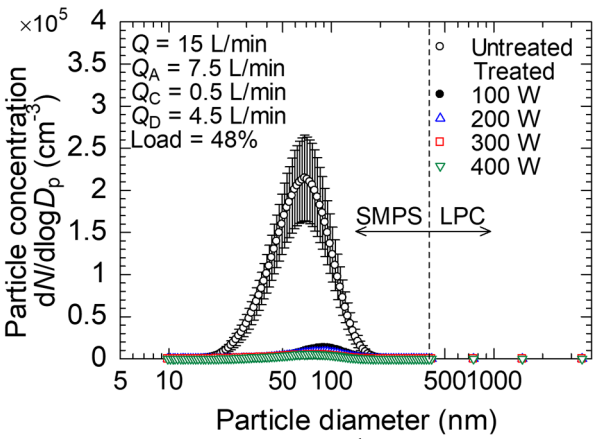

(f) flow rate Q of 15 L min^{-1}, engine loads of 48 %.

Fig. 3. Particle concentration before and after plasma treatment for flow rates of 5–15 L min^{-1}, engine loads of 0 & 48%. The white symbol indicates particle concentration before treatment, and the colored symbols indicate the particle concentration after treatment with input power of 100, 200, 300, and 400 W. Each symbol and error bar represent the average value of the measurements and the standard deviation $\pm\sigma$, respectively.

Each symbol indicates the particle number concentration before treatment and after treatment at input powers of 100 W, 200 W, 300 W, and 400 W. Measurements are performed four times under the same conditions, and the error bars in each plot indicate the standard deviation. The dotted line indicates the change in measurement range between SMPS and LPC. Measurements are performed in the range of 9.82–414.2 nm for SMPS and 400–3500 nm for LPC. The measurement results show that the plasma reactor exhibits high performance in PM removal. As the engine load increases, the particle size at the peak of the particle number concentration distribution before treatment becomes larger, and the proportion of particles with large diameters increases. The possible reason for this is as follows: PM is generated when organic components such as soluble organic fraction (SOF) adhere to the aggregates formed by the aggregation of soot particles. It is thought that the increase in load makes it easier to generate more soot particles, SOF, and aggregates, which leads to an increase in particles with large diameters. In addition, the increase in load increases the combustion temperature of the engine, which burns fine particles. The combustion of fine particles increases the proportion of particles with large diameters.

3.2 Particle removal efficiency

Fig. 4 shows the average PM removal efficiency by flow rate and engine load. Fig. 4 (a) shows the measurement results at a flow rate of 5 L min^{-1} and 0% load, Fig. 4 (b) shows the measurement results at a flow rate of 5 L min^{-1} and 48% load, Fig. 4 (c) shows the measurement results at a flow rate of 10 L min^{-1} and 0% load, Fig. 4(d) shows the measurement results at a flow rate of 10 L min^{-1} and 48% load, Fig. 4 (e) shows the measurement results at a flow rate of 15 L/min and 0% load, and Fig. 4 (f) shows the measurement results at a flow rate of 15 L min^{-1} and 0% load. The horizontal axis shows the particle size (nm), and the vertical axis shows the removal efficiency (%). The flow rates of Q, Q_A, Q_C, and Q_D are the same as those in Fig. 3. Measurement times, and the meanings of the error bars and the dotted lines in the figure are the same as those in Fig. 3. Data is excluded when the number of particles before treatment is less than 1/100 of the peak value of the particle number concentration distribution for each particle size. When the number of particles before treatment is small, the ratio of the number of particles after treatment to the number of particles before treatment increases, resulting in a large measurement error. Removal efficiencies of 92% or more, 86% or more, 79% or more, 76% or more, 77% or more, and 71% or more are achieved for all particle sizes under the conditions of 5 L min^{-1} flow rate, 0% load, 5 L min^{-1} flow rate, 48% load, 10 L min^{-1} flow rate, 0% load, 10 L min^{-1} flow rate, 48% load, 15 L min^{-1} flow rate, 0% load, 15 L min^{-1} flow rate, 48% load, respectively. As the reactor power increases, the number of small particles increases, and the removal efficiency decreases in the small particle size range. It is considered that the combustion of larger particles is converted into smaller particles, resulting in an increase in the number of smaller particles.

3.3 PM removal efficiency for various specific energy

Fig. 5 shows the calculation results of PM removal efficiency against input energy per unit volume (Specific Energy (*SE*)). The horizontal axis shows *SE* (J/L), and the vertical axis shows PM removal efficiency (%). The symbols show removal efficiency at loads of 0%, 24%, 48%, and 72%, respectively. From the figure, a removal efficiency of 83% or more is obtained under all flow rate, load, and input power conditions. Removal efficiency of 95% or more is obtained under flow rate conditions of 5 and 10 L min^{-1}. When the flow rate is small, the residence time of the mixed gas in the reactor is long, so sufficient treatment is performed by discharge. When the flow rate is 15 L min^{-1}, the removal efficiency decreases under lower *SE* and lower load conditions. Under these conditions, the residence time is short due to the high flow rate, PM concentration becomes larger, and the discharge power is small. In our previous study [39], a removal efficiency of 98% or more is achieved at a flow rate of 5 L min^{-1}. In this study, a low-emission diesel engine is used, which emits small amounts of particulate matter. At flow rates of 5 and 10 L min^{-1}, a removal efficiency of over 95% is achieved, and sufficient treatment is achieved compared with previous studies.

In the experiment, NO_x in the exhaust gas was reduced and removed by reacting with HC and CO in the exhaust gas. At a power of 100 W, the exhaust gas reached a temperature of approximately 80°C; under such condition the reduction reaction exceled NO_x generation by the plasma. The removal efficiency of THC was almost constant irrespective of *SE* because the exhaust gas contains a certain concentration of hydrocarbons which are difficult to be decomposed by the plasma, such as monocyclic and polycyclic aromatic hydrocarbons. At a flow rate of 15 L min^{-1} and power of 100 W, the highest performance in simultaneous removal of 96%

PM, 67% NO_x, and 76% HC were confirmed. Note that these are reference data indicating the possibility of simultaneous removal, and detailed experiments are currently underway. The exhaust gas treatment system can achieve a high treatment performance when operated at low *SE*.

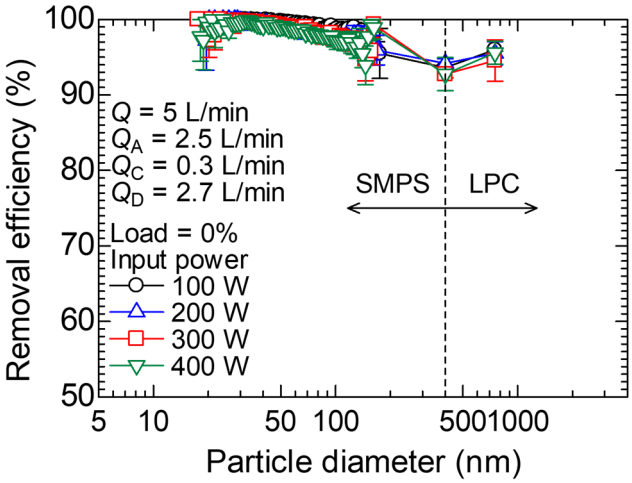

(a) flow rate Q of 5 L min^{-1}, engine loads of 0%.

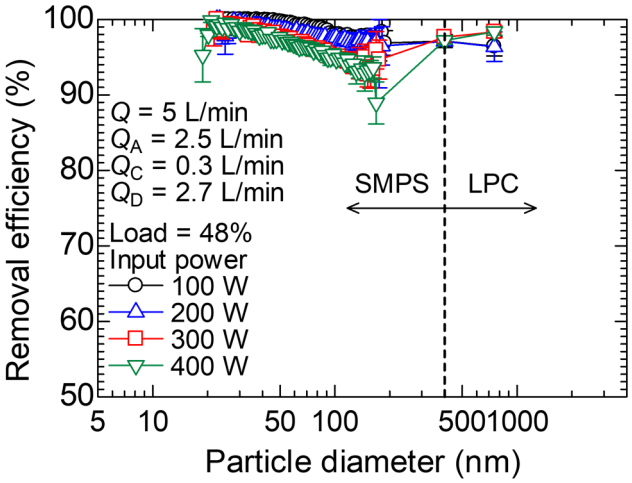

(b) flow rate Q of 5 L min^{-1}, engine loads of 48%.

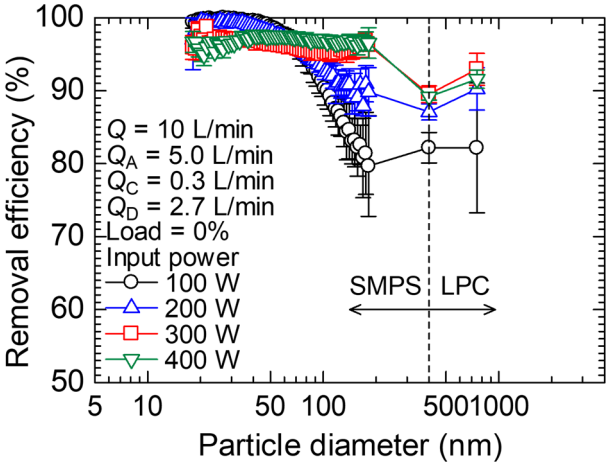

(c) flow rate Q of 10 L min^{-1}, engine loads of 0%.

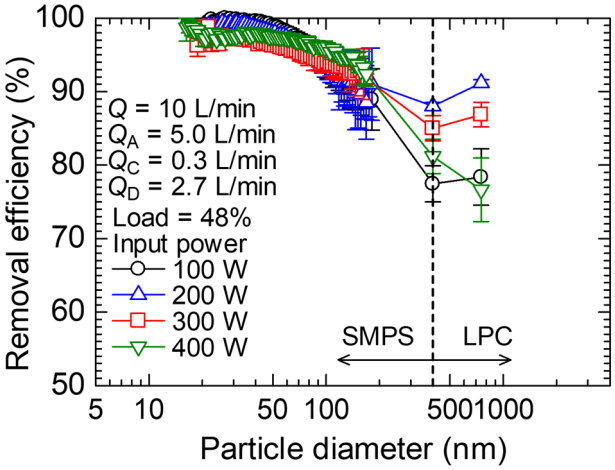

(d) flow rate Q of 10 L min^{-1}, engine loads of 48%.

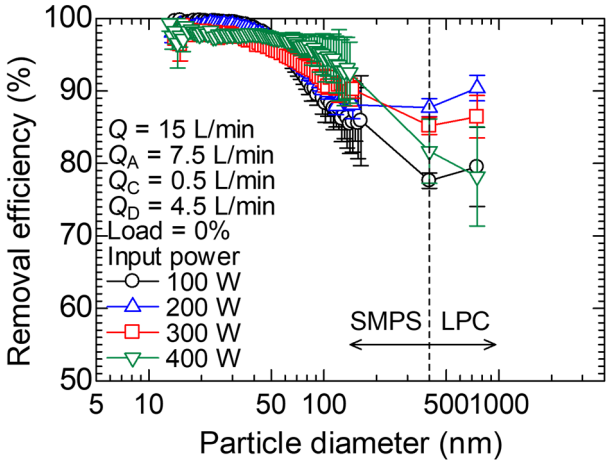

(e) flow rate Q of 15 L min^{-1}, engine loads of 0%.

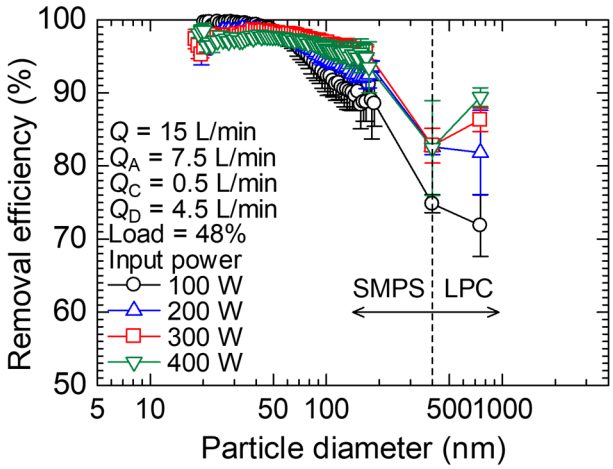

(f) flow rate Q of 15 L min^{-1}, engine loads of 48%.

Fig. 4. Particle removal efficiency. Symbols indicate the average removal efficiency after treatment with input power of 100, 200, 300, and 400 W.

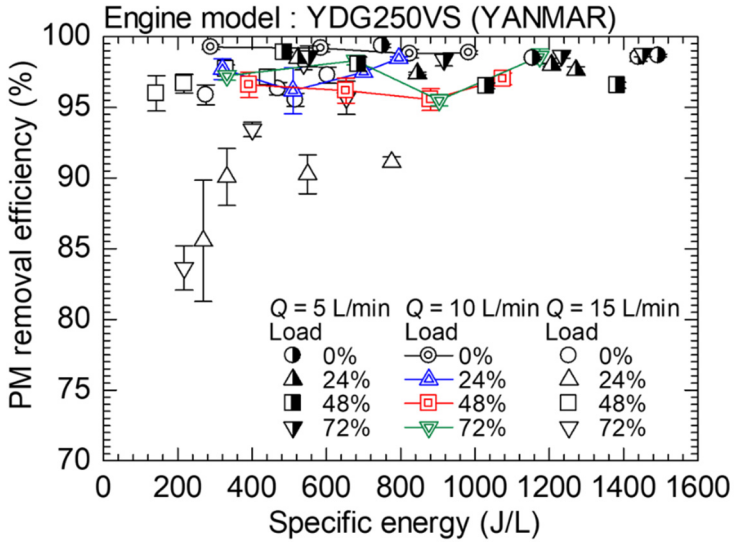

Fig. 5 PM removal efficiencies for specific energy. Symbols indicate the removal efficiencies for various conditions.

4. Conclusion

The inferences obtained in this study are summarized below:

(1) The removal efficiency of PM against *SE* is 83% or more under all flow rate, load, and input power conditions. PM is removed by oxidation and combustion by atomic oxygen species generated by the surface discharge plasma.

(2) In this study, a low-emission diesel engine with low particulate emissions is used, and a removal efficiency of 95% or more is achieved under flow rates of 5 and 10 L min^{-1}, which is sufficient as compared with the previous study. When the flow rate is 15 L min^{-1}, the removal efficiency decreases under lower *SE* and lower load conditions. Under these conditions, the residence time is short due to the high flow rate, PM concentration becomes larger, and the discharge power is small.

(3) In the particle number concentration distribution of PM by size before and after treatment by flow rate and engine load, as the input power of the reactor increases, the proportion of large particles decreases due to the combustion of large particles, and the proportion of small particles increases, resulting in a smaller peak particle size after treatment. It is considered that as the input power increased, larger particles are combusted and changed into smaller particles.

(4) In terms of the average PM removal efficiency by flow rate and engine load, as the reactor power increase, the number of small particles increases, and the removal efficiency decreases in the small particle size range. It is considered that as the large particles are combusted, they are changed into smaller particles, and the number of small particles increases. There is a possibility that this surface discharge electrostatic reactor can achieve highly efficient simultaneous removal of PM, NO_x, and hydrocarbons. The detailed experiments are currently underway.

Acknowledgment

This study was partially supported by JSPS KAKENHI Grant Number JP23H01626.

References

[1] Okubo M., Recent development of technology in scale-up of plasma reactors for environmental and energy applications, *Plasma Chem. Plasma Process.,* Vol. 42, pp. 3–33, 2022.

[2] Hattori Y., Improvement of thermal efficiency and exhaust emission in diesel engine by applying spray internal EGR (Fifth report), *Trans. JSME*, Vol. 52 (3), pp.530–535, 2021.

[3] Nishizawa T., Study of improvement for combustion stability under cold start condition of DI diesel engine (First report), *Trans. JSME*, Vol. 44 (4), pp. 989–994, 2013.
[4] Kuwahara T., Yoshida K, Kuroki T, Hanamoto K, Sato K, and Okubo M., Pilot-Scale combined reduction of accumulated particulate matter and NO_x using nonthermal plasma for marine diesel engine, *IEEE Trans. Ind. Applicat.,* Vol. 56 (2), pp.1804–1814, 2020.
[5] Kim H.J., Kim M., Han B., Woo C.G., Zouaghi A., Zouzou N., and Kim Y.J., Fine particle removal by a two-stage electrostatic precipitator with multiple ion-injection-type prechargers, *J. Aerosol. Sci.,* Vol. 130, pp. 61–75, 2019.
[6] Kim M., Lim G.T., Kim Y.J., Han B, Woo C.G., and Kim H.J., A novel electrostatic precipitator-type small air purifier with a carbon fiber ionizer and an activated carbon fiber filter, *J. Aerosol. Sci.,* Vol. 117, pp. 63–73, 2018.
[7] Mokhri M., Abdullah N., Abdullah S., Kasalong S., and Mamat R., Soot filtration recent simulation analysis in diesel particulate filter (DPF), *Procedia Eng*., Vol. 41, pp.1750–1755, 2012.
[8] Okubo M. and Kuwahara T., New Technologies for Emission Control in Marine Diesel Engines: Butterworth-Heinemann, imprint of Elsevier, 2019.
[9] Palma V., Ciambelli P., Meloni E., and Sin A., Catalytic DPF microwave assisted active regeneration, *Fuel,* Vol. 140, pp. 50–61, 2015.
[10] Palma V., Ciambelli P., Meloni E., and Sin A., Study of the catalyst load for a microwave susceptible catalytic DPF, *Catal. Today,* Vol. 216 (6), pp.185–193, 2013.
[11] Huang Y., Ng E.C.Y., Surawski N.C., Zhou J.L., Wang X., Gao J., Lin W., and Brown R.J., Effect of diesel particulate filter regeneration on fuel consumption and emissions performance under real-driving conditions, *Fuel*, Vol. 320, 123937, 2022.
[12] Okubo M., Arita N., Kuroki T., Yoshida K, and Yamamoto T., Total diesel emission control technology using ozone injection and plasma desorption, *Plasma Chem. Plasma Process.,* Vol. 28 (2), pp. 173–87, 2008.
[13] Babaie M., Davari P., Talebizadeh P., Zare F., Rahimzadeh H., and Ristovski Z., *Chem. Eng. J*, Vol. 276 (2), pp. 240–248, 2015.
[14] Pu X., Cai Y., Shi Y., Wang J., Gu L., Tian J., and Fan R., Carbon deposit incineration during engine flameout using non-thermal plasma injection, *Int. J. Automot. Technol.,* Vol. 19, pp. 421–432, 2018.
[15] Ranji-Burachaloo H., Masoomi-Godarzi S., Khodadadi AA., and Mortazavi Y., Synergetic effects of plasma and metal oxide catalysts on diesel soot oxidation, *Applicat. Catal. B: Environ.,* Vol. 182, pp. 74–84, 2016.
[16] Ji L., Cai Y., Shi Y., Fan R., Wang W., and Chen Y., Effects of nonthermal plasma on microstructure and oxidation characteristics of particulate matter, *Environ. Sci. Technol.,* Vol. 54, pp. 2510–2519, 2020.